Stimulated Raman measurements of the hyperfine structure in Y II

T. P. Dinneen, N. Berrah Mansour, C. Kurtz, and L. Young
Physics Division, Argonne National Laboratory, Argonne, Illinois 60439
(Received 26 October 1990)

Stimulated Raman spectroscopy has been used in a fast ion beam to measure the hyperfine structure in the $4d^2$ configuration of Y II. A simple theory is provided for the line shape of the coherent two-photon transition which gives a transit-time limited linewidth of $0.9/T$, comparable to the resolution of the laser–radio-frequency double-resonance technique. The hyperfine structure is compared with a multiconfiguration Dirac-Fock calculation and with that of the homologous Sc II ion. This comparison confirms the role of core polarization as a significant factor in the hyperfine structure of these ions.

INTRODUCTION

Stimulated Raman or coherent two-photon spectroscopy has received much attention in recent years both for its potential to make high-precision measurements[1-3] and for its use in frequency standards.[4,5] For radio-frequency (rf) precision spectroscopy in ion beams, it is intrinsically different from the well-established laser-rf double-resonance technique in that the rf signal is applied to the laser beam and not the ion beam. This turns out to be a clear advantage at low frequencies (<50 MHz in our apparatus) where the rf signal, when applied to the ion beam, perturbs the ion motion.[6] In removing the rf from the ions this low-frequency limitation is removed. The all optical Raman process has made possible the measurement of the hyperfine structure (hfs) intervals in singly ionized yttrium that were previously impossible. In the stimulated Raman process to be described in this paper, two long-lived lower states and one excited state are involved in the optical transitions. At exact two-photon resonance, a fraction of the population becomes trapped in the two lower states. This trapping is detected as a loss of spontaneous-decay fluorescence from the upper state. As in the laser-rf double-resonance method a direct measurement is made on the lower state splitting with transit-time limited precision.

We report in this paper the first measurements of the hfs of four levels in the metastable $4d^2$ configuration of Y^+. Three of the four levels required the use of the stimulated Raman process because of incomplete optical resolution due primarily to the small spin and magnetic moment of the yttrium nucleus. The resolution of the two-photon process used in these measurements is assessed from a simple model, which is detailed in the Appendix. The systematic errors involved are estimated and a comparison is made with the double-resonance technique. The results of the hfs measurements in the $[Kr]4d^2$ configuration of Y^+ are also compared with *ab initio* multiconfiguration Dirac-Fock (MCDF) calculations. Our previous studies[7] in the $[Ar]3d^2$ configuration of Sc^+ revealed a major disagreement with MCDF calculations, interpreted to be due to the polarization of the [Ar] core by the two valence electrons. Our current measurements in Y^+ show the trend to increasing core polarization from [Ar] to [Kr].

APPARATUS

The apparatus for the laser-rf double resonance has been described in detail previously and basically consists of an ion source, accelerator, mass analyzer, and a series of optical and rf interaction regions.[6,7] For the stimulated Raman work we improved our optical detection system by installing a magnetically shielded 30-cm-long laser interaction region at the end of the beamline, as shown in Fig. 1. The device has an elliptic cross section, the interior surface being of polished aluminum with greater than 80% reflectivity down to 300 nm. A 2-cm hole in the end pieces at one of the foci allows for entry and exit of the laser and ion beam. The result is a large solid angle coverage for scattered radiation. The ions and laser interact along one focal line of the device and the scattered fluorescence is collected at the other by two area-conserving light pipes which convert the 30 cm $\times 0.64$ cm line image into two square sections, 3.1 cm on a side, that match a photomultiplier's active area. The solid light pipe has a wavelength cutoff at 360 nm but can be used below this wavelength by coating the entrance with a thin layer of sodium salicylate[8,9] wave shifter. Sodium salicylate absorbs efficiently below 350 nm and reemits in a band around 420 nm.

The two optical frequencies needed for the Raman process are generated by passing the output of a dye laser through a $LiTaO_4$ electro-optic crystal across which rf signal is applied. A fraction of the laser power is shifted into optical sidebands $\pm\omega_{rf}$ from the central laser frequency. The frequency offset of the sideband is accurately controlled by an Adret model 742A synthesizer. The above technique results in optical fields with correlated frequency jitter, which means that the rms laser linewidth (1 MHz) does not limit the linewidth of the two-photon resonance.

In the current study, ions in the metastable $4d^2$ configuration were laser excited to the intermediate $4d5p$ configuration with 560-nm laser light. The 320-nm decay to the ground $4d5s$ configuration was detected using the

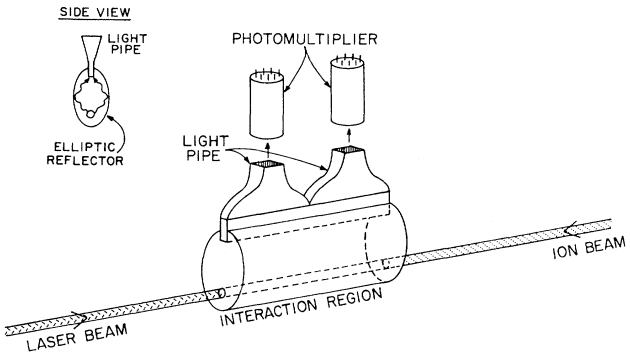

FIG. 1. Schematic of the laser–ion-beam interaction region showing the light collection system. The interior of the ellipse is a polished aluminum surface. The laser-ion interaction occurs along one of the focal lines of the ellipse and the scattered light is collected at the other.

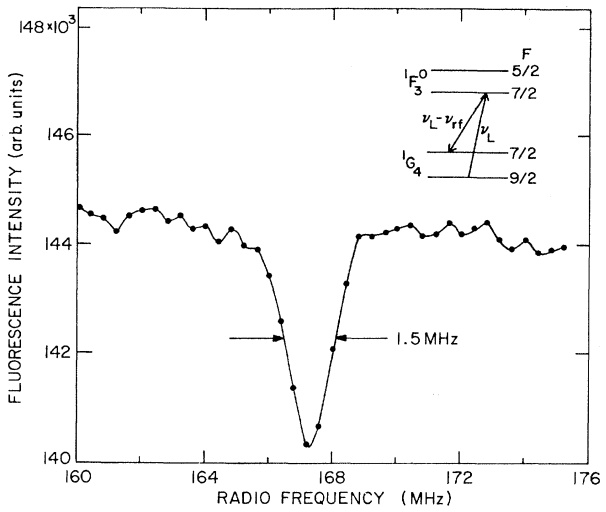

FIG. 3. Stimulated Raman resonance spectrum showing the loss of fluorescence at the two-photon resonant frequency. The frequency scale on the axis corresponds to the difference between the two optical frequencies. The inset shows the transitions involved in the measurement.

wave-shifting technique followed by an interference filter at the photomultiplier to discriminate against scattered laser light.

EXPERIMENTAL METHOD

The fast ion beam provides a kinematic compression of the Doppler linewidth in the optical spectrum which, for many ions, is sufficient to determine the dipole term of the hyperfine interaction. However, in the case of yttrium the spectra are not completely resolved due to the small nuclear dipole moment. A laser-induced fluorescence spectrum of the Y II $4d^2\ {}^1G_4 \rightarrow 4d5p\ {}^1F_3^\circ$ transition is shown in Fig. 2. The nuclear spin of yttrium is $\frac{1}{2}$ and three lines are expected in a fully resolved hyperfine pattern of this transition. Though incompletely resolved it is possible to determine that the level structure is inverted and, to within ±20 MHz, the magnitudes of the lower and upper state splittings. Typical Doppler linewidths found were 70 MHz [full width at half maximum (FWHM)] or more for all of the optical transitions measured in yttrium. This width was larger than expected based on previous experience[7] and indicates a large energy spread (≈10 eV) from the ion source. Narrow linewidths are almost always essential[10] for selective and efficient optical pumping in laser-rf double resonance. Here the small hfs coupled with this poor resolution made double resonance essentially impossible.

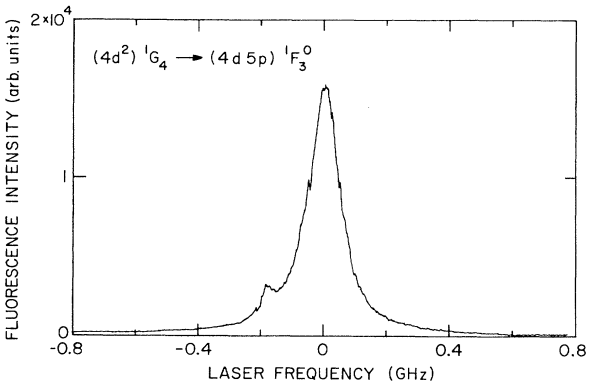

FIG. 2. Laser-induced fluorescence frequency scan of the $4d^2\ {}^1G_4$-$4d5p\ {}^1F_3^\circ$ transition. The two strong hyperfine components of this transition are unresolved in this spectrum, the third weak component is visible on the left.

The stimulated Raman technique does not require the same initial optical resolution and does not perturb the ion beam at low radio frequencies, making it a good replacement for double resonance in these cases. To make a measurement the central laser frequency is fixed on resonance with one hyperfine component of the optical transition and the sideband is scanned over another hyperfine component, both components sharing a common upper level. The decay fluorescence out of the three-level system from the excited state to the ground state is the detected signal. At exact two-photon resonance a dip is seen in the fluorescence signal corresponding to trapping in the lower state. Figure 3 shows a stimulated Raman spectrum of the $^1G_4$ level showing the decrease in fluorescence at two-photon resonance. The background is the sum of the fluorescence due to the two independent optical transitions. Typical dip sizes ranged from 1% to 5% of the total fluorescence for all of the lines measured in yttrium while the linewidths varied from 1 to 2 MHz.

COMPARISON WITH MODEL

The simple model of the interaction, as described in the Appendix, can be used to extract an estimate of the linewidth and signal size expected. These parameters can then be optimized for each transition studied. The main

results are outlined below and compared with the experimental observations on the $^1G_4$ level.

The linewidth (FWHM) can be found by numerical evaluation of Eq. (A8) in the Appendix to be approximately $0.9/T$ (Hz), in the low-laser-power limit, where T is the ion transit time. The transit time is 0.9 μs for 50-kV yttrium ions through the 30-cm region, giving an estimated linewidth of 1 MHz. The comparable expression for the laser-rf double-resonance linewidth is $0.8/T$. The upper section of Fig. 4 shows the measured linewidth of the Raman transition as a function of laser-power density. For these measurements only the first photomultiplier in the detection region was operational and, since light is gathered preferentially from the first half of the interaction region, the detector sees an increased linewidth from the lower effective transit time. The solid line immediately below the data is the expected linewidth assuming both photomultipliers are used. A few measurements were made with both photomultipliers active and are about 200 kHz narrower, in better agreement with the theoretical line.

The signal size, as estimated from Eq. (A8), is not as well defined and depends greatly on the initial populations of the states, relative strengths of the transitions, and the laser power. In the infinite time limit, and with equal initial populations, 50% of the population should be trapped at exact resonance regardless of the laser powers on the two transitions. However, for short interaction times and fixed total laser intensity, optimal trapping should occur in the cases where the Rabi frequencies for both transitions are comparable, though not necessarily equal. The actual measurements on the $^1G_4$ level in yttrium do not show any dependence of the signal size on laser power, in disagreement with the simple theory. An explanation for this difference is found in the added complications of near-resonant interactions with nearby levels. For this specific case of $^1G_4$ there is a near degeneracy of the two $^1G_4 \rightarrow {}^1F_3^\circ$ $\Delta F = -1$ hyperfine components as can be seen in Fig. 2. The existence of this near-resonant transition, which is unrelated to the three-level process under investigation, allows for a leak of the trapped population and thereby a loss of the Raman signal. The initial tests of the Raman technique on the scandium ion[6] were performed on the $^3P_2 \rightarrow {}^3P_2^\circ$ transition, where there are no nearby resonances and the three-level theory should be a much better model. In this case the signals depended greatly on laser power with a maximum up to 40% of the background fluorescence being lost at two-photon resonance. Although this transition was a much better candidate for testing the technique, the interaction region used at the time was not suited for such measurements and the laser powers used exceed the approximations used in the Appendix. Despite the fact that the Y II $^1G_4 \rightarrow {}^1F_3^\circ$ transition does not truly provide a three-level system, the resolution of the process remains as the simple theory would predict.

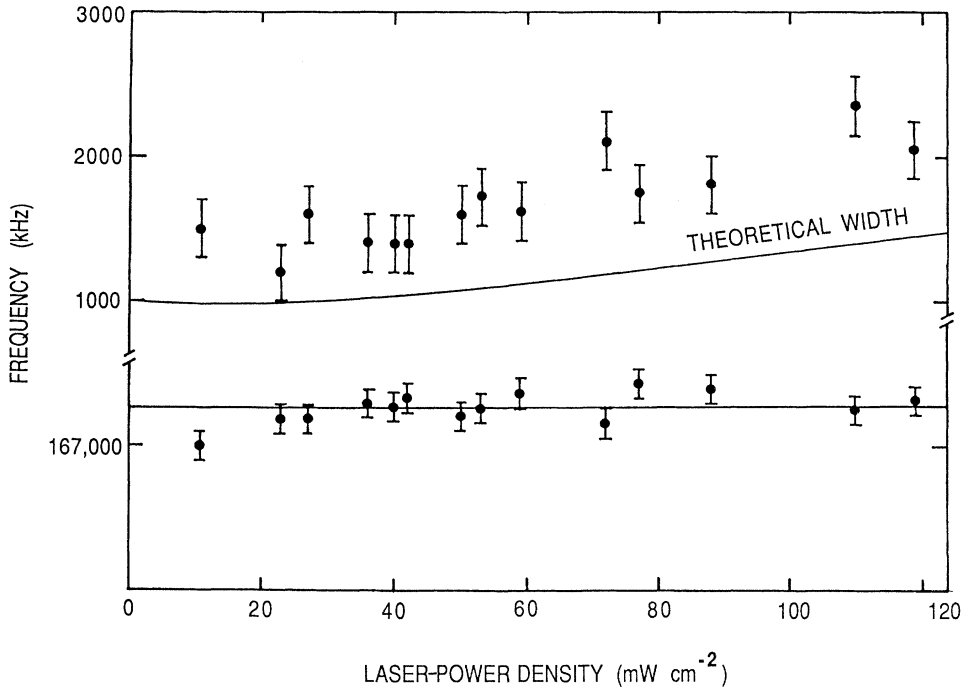

FIG. 4. The upper part of this figure shows the measured linewidth of the Raman transition as a function of power. For these measurements only one of the photomultipliers shown in Fig. 1 was active. The solid line immediately below the data is the result of a numerical evaluation of Eq. (A8) in the Appendix. The lower part of the figure shows the two-photon transition frequency as a function of laser power.

TABLE I. The measured hyperfine intervals in the metastable $4d^2$ configuration and a comparison with theory. The negative signs on the measurements imply the structure is inverted. The $^3P_1$ level was measured by double resonance that resulted in a smaller uncertainty. The $^3P_2$ has potentially large light shifts due to the small laser detunings involved.

Level	$F \rightarrow F+1$	Experiment	MCDF
$4d^2\ ^1G_4$	$\frac{7}{2} \rightarrow \frac{9}{2}$	−167.4(2)	−172.5
$4d^2\ ^1D_2$	$\frac{3}{2} \rightarrow \frac{5}{2}$	−66.0(2)	−55.4
$4d^2\ ^3P_1$	$\frac{1}{2} \rightarrow \frac{3}{2}$	69.84(2)	3.7
$4d^2\ ^3P_2$	$\frac{3}{2} \rightarrow \frac{5}{2}$	29(1)	−97.7

RESULTS

Table I shows the results for the four metastable levels measured and a comparison with a MCDF (Ref. 11) calculation. Negative signs have been given to those measurements where the initial optical spectra showed the level to be inverted, or where a combination of the optical and rf spectra implied an inverted structure. The negative signs are to be expected from the known negative dipole moment of yttrium. [$\mu_I = -0.137\ 33$ n.m. (n.m. denotes nuclear magneton).] A major success of the stimulated Raman technique can be seen in the measurement of the $4d^2\ ^3P_2$ level hyperfine splitting of 29 MHz. Our previous attempts[6] to measure such small splittings by laser-rf double resonance perturbed the ion trajectories so much that measurements were impossible.

Table II shows the hyperfine (A) constants derived for yttrium along with those of the homologous scandium ion. It can be seen that the MCDF predictions for the triplet levels do not agree well with the measurements in both ions. In our previous study of Sc II the Sandars-Beck[12] effective operator approach was used to show the presence of a large contact contribution to the hfs. It was concluded that the origin of this term lay in core polarization. Here again we analyze the hfs in terms of these effective operators. The magnetic dipole interaction for a single valence electron is written

$$H_{\rm hfs} = [a_{nl}^{01}\mathbf{l} - \sqrt{10}\,a_{nl}^{12}(\mathbf{s}^{(1)} \times \mathbf{C}^{(2)})^{(1)} + a_{nl}^{10}\mathbf{s}] \cdot \mathbf{I} \qquad (1)$$

where the a_{nl} are various radial integrals. In the nonrelativistic limit $a_d^{01} = a_d^{12}$ and $a_d^{10} = 0$. Any interaction that produces a contact contribution will appear as a change in a_d^{10} and relativistic corrections cause a^{01} and a^{12} to differ. In this analysis we set $a^{01} = a^{12}$, allow a^{10} to vary, and achieve a good fit to the data. The results for yttrium give $a^{01} = -34$ MHz and $a^{10} = 79$ MHz. The contact contribution a^{10} is again seen to be quite large and more characteristic of s electrons, indicating that core polarization is also important in yttrium. The analysis using Eq. (1) assumes LS coupled states in contrast to the MCDF calculations which include many configurations. However, the empirical fit allows for core polarization which is not included in the MCDF calculation. Core polarization arises from the Coulomb interaction between open shell valence electrons and core electrons. The exchange interaction results in electrons of the same spin acquiring an attractive component to their interaction. Some nonrelativistic calculations have been made which allow for this interaction. Spin-polarized Hartree-Fock (SPHF) calculations, in which the radial functions are allowed to depend on the spin, show the effect of an increased contact contribution in systems with d valence electrons.[13] Watson and Freeman[14] show the results of a series of calculations on the neutral $3d$ series atoms and the doubly ionized $3d$ and $4d$ series. The metastable levels in our singly ionized systems have the same core as the doubly ionized systems calculated and so would be expected to show a similar electron spin density at the nucleus. Calculating this spin density from

$$\chi = \frac{4\pi}{2S}|\psi(0)|^2 \quad \text{with } a^{10} = \frac{16\pi}{3}\frac{\mu_I}{I}\mu_N\mu_B|\psi(0)|^2\ ,$$

where S is the spin, results in $\chi(\text{Sc}\ 3d^2) = -1.3$ a.u. and $\chi(\text{Y}\ 4d^2) = -2.3$ a.u. compared with the calculated values of -3 and -8 a.u. for the doubly ionized species, respectively. It is clear from the calculations that large contact interactions can be achieved and play an important role in the hyperfine interaction. However, even in these nonrelativistic calculations there are severe convergence problems which result from the relaxation of constraints in the Hartree-Fock calculations. No comparable relativistic calculations have yet been made on these systems.

TABLE II. Hyperfine A values for both yttrium and scandium in the d^2 configuration. $A_{(\rm expt)}$ are experimental values and $A_{\rm MCDF}$ are theoretical values. In each case it can be seen that the singlet values are in better agreement with theory but that the triplet levels are not.

Level	Sc^+ $A_{(\rm expt)}$	$A_{\rm MCDF}$	Y^+ $A_{(\rm expt)}$	$A_{\rm MCDF}$
$^1G_4$	135.23	143.2	−37.20	−38.3
$^1D_2$	149.36	146.6	−26.40	−22.2
$^3P_1$	−107.50	−1.8	46.56	2.5
$^3P_2$	−27.73	85.9	11.60	−39.1

LIGHT SHIFTS

A comparison of the uncertainties in Table I shows that the precision of the laser-rf double-resonance measurement on the $^3P_1$ level is a factor of 10 better even though both techniques have an equivalent theoretical resolution. One reason for this difference is the lack of statistics in the current measurements due to losses caused by nearby levels; another is the systematic error that arises from light shifts.[15,16] Both of these are inherent to the present system and not to the technique. The presence of a near-resonant laser transition, which connects one of the lower levels being measured to an excited level which is not part of the three-level system, will cause an ac Stark shift of the levels being measured. Laser-rf double resonance allows this to be overcome because it consists of three separated sections for the optical and rf interactions. Doppler tuning of the ion beam out of optical resonance in the rf section reduces the light

shifts. In comparison, the stimulated Raman method does not have this feature and relies on the atomic levels to be well spaced to avoid light shifts.

The existence of nearby levels necessitates the use of the lowest laser powers possible in order to reduce light shifts. Figure 5(a) shows the effect of the extra laser sideband on a three-level system. The detuning from resonance is shown for each level and the resulting ac Stark shift of the lower levels sets a limit on the precision of the measurement in this system. Figure 5(b) shows the effect of a fourth level on a two-photon transition. Here the $^1G_4(F=\frac{7}{2}, \frac{9}{2})$ and $^1F_3^\circ(F'=\frac{7}{2})$ make up the three-level system under investigation. The detuning of the lasers from the $F=\frac{7}{2}$ to $F'=\frac{5}{2}$ transition are shown which, again, causes an ac Stark shift of the lower $F=\frac{7}{2}$ level. All combinations of these two processes are taken into account in calculating the light shifts. Table III shows the light shift contributions due to the extra levels and laser sidebands. The calculation is for the $m_f=\frac{3}{2}$ sublevel assuming linear polarization of the laser beams. The $^1G_4$ $F=\frac{9}{2}$ level is perturbed only by the presence of the second laser sideband while the $F=\frac{7}{2}$ level is perturbed by interactions with both the $^1F_3^\circ$ $F'=\frac{5}{2}$ level and the second laser sideband.

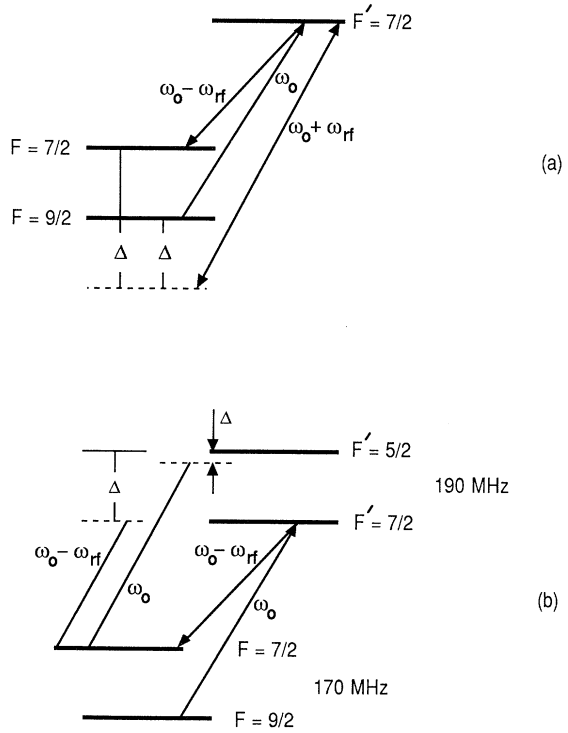

FIG. 5. (a) shows the detuning of the second laser sideband from resonance. Here, both of the lower levels are perturbed due to the nonresonant interaction. (b) shows the effect of the $F'=\frac{5}{2}$ level on the Raman measurement. The detunings of the two lasers from resonance with the $F=\frac{7}{2}\rightarrow F'=\frac{5}{2}$ are shown by the dotted lines. The $F=\frac{9}{2}$ level is not affected as there is no optical transition to the $F'=\frac{5}{2}$ level.

TABLE III. Contributions to the light shift from near-resonant interactions. The upper part of the table shows all the perturbations to the $^1G_4$ $F=\frac{7}{2}$ level due to nonresonant interactions with the $F'=\frac{5}{2}, \frac{7}{2}$ levels of the $^1F_3^\circ$ state. The lower part of the table gives the perturbations on the lower $F=\frac{9}{2}$ level. These combine to produce a total shift of 98.6 (kHz). These values are for power densities of 5 mW/cm^2 on the $^1G_4(F=\frac{7}{2})\rightarrow{}^1F_3^\circ(F=\frac{7}{2})$ transition and 10 mW/cm^2 for the return transition to the $^1G_4(F=\frac{9}{2})$ level.

F	F'	Detuning (MHz)	$(\omega_r)^2$ (10^{12} s^{-2})	Shift (kHz)
$\frac{7}{2}$	$\frac{5}{2}$	−150	352.0	15.4
	$\frac{7}{2}$	−340	3.9	0.0
	$\frac{5}{2}$	190	352.0	−12.2
	$\frac{5}{2}$	20	352.0	−87.0
$\frac{7}{2}$	Total shift			−83.8
$\frac{9}{2}$	$\frac{7}{2}$	−170	383.3	14.8

The ac Stark shift, being magnetic sublevel dependent, should broaden the transition as well as shift the transition frequency. When the calculations shown in Table III are repeated for other magnetic sublevels, it is found that the total shift of the resonance frequency varies from 10 kHz, for the $|m_F|=\frac{7}{2}$ sublevel, to 120 kHz, for the $|m_f|=\frac{1}{2}$ sublevel. Thus the transition would be expected to broaden at higher laser powers. A full multilevel calculation would need to be done to reliably determine the contribution of each of the sublevels to the observed signal and hence to correct for the light shift. The experimental solution to the light shift problem is to measure the position of the resonance as a function of laser power and extrapolate to zero power. Figure 4 shows the width and position as a function of laser power. The transition width is expected to increase with laser power based on the simple three-level theory as stated in the Appendix and little can be implied from the width, however there is no real evidence of light shifts affecting the position within the experimental uncertainty. The errors as quoted in Table I are not the experimentally determined uncertainties but represent the largest calculated light shift for each transition based on the lowest laser power used.

CONCLUSION

We have used the stimulated Raman process to determine the hyperfine structure in the $4d^2$ configuration of Y II. The precision of this technique has been shown to compare favorably with the well-known laser-rf double-resonance technique. The experimental magnetic-dipole (A) hyperfine interaction constants have been compared with a MCDF calculation and, as in our previous studies with the homologous Sc II ion, the singlet levels are found to be in good agreement while the triplet levels are not. This disagreement with theory has been attributed to polarization of the atomic core by the open shell electrons. Nonrelativistic spin-polarized HF calculations do exist

for the doubly ionized $3d$ and $4d$ ions which find large electronic spin densities at the nucleus comparable to those found in these singly ionized ions. These calculations have not been extended to the relativistic MCDF calculations.

ACKNOWLEDGMENTS

We thank U. Nielsen for the MCDF calculations. This research was supported by the U.S. Department of Energy, Office of Basic Energy Sciences, under Contract No. W-31-109-ENG-38.

APPENDIX: THREE-LEVEL SYSTEMS

Many authors have used the density matrix approach to describe the behavior of the three-level system. An exact analytic solution of the coupled equations is not available and numerical integration is not very illuminating. Various approximations have been used by these authors which allow analytic solutions, and give some insight into the problem.[4,17,18] One such case is when the decay rate out of the system is very large, as in our studies where the two lower states are metastable and the intermediate excited state decays preferentially to the ground state. With this simplification the quantum-mechanical amplitude approach of Hemmer *et al.*[4] is expected to give a good description of the process.

Our interest in this approach is to extract an estimate of the linewidth and size of the expected signal in our apparatus. The notation is that of Hemmer and begins with writing the wave function in the interaction representation, using a classical electric field $E(\mathbf{x},t)$ and a phenomenological term, γ_2, to account for the spontaneous decay out of the three-level system:

$$\Psi(\mathbf{x},t)=\sum_j a_j(t)U_j(\mathbf{x})\exp(i\varepsilon_j/\hbar)t \quad \text{with } j=1,2,3 \ , \tag{A1}$$

$$E(\mathbf{x},t)=\tfrac{1}{2}[E_1(\mathbf{x})\exp(-i\omega_1 t)+E_2(\mathbf{x})\exp(-i\omega_2 t)]+\text{c.c.} \tag{A2}$$

where U_j is the wave function of state j, ε_j is the energy, and $|a_j(t)|^2$ is the probability of finding the atom in state j at some time t. Substituting these expressions into the Schrödinger equation results in the following amplitude equations:

$$\dot{a}_1=\tfrac{1}{2}i\Omega_1^*\exp(i\delta_1 t)a_2 \ , \tag{A3}$$

$$\dot{a}_2=\tfrac{1}{2}[i\Omega_1\exp(-i\delta_1 t)a_1 + i\Omega_2\exp(-i\delta_2 t)a_3-\gamma_2 a_2] \ , \tag{A4}$$

$$\dot{a}_3=\tfrac{1}{2}i\Omega_2^*\exp(i\delta_2 t)a_2 \ , \tag{A5}$$

where $\Omega_{1,2}$ are the Rabi frequencies of the optical transitions and $\delta_1=\omega_1-(\varepsilon_2-\varepsilon_1)/\hbar$ and $\delta_2=\omega_2-(\varepsilon_2-\varepsilon_3)/\hbar$ are the detunings from exact resonance of the two optical fields. Levels 1 and 3 are the two lower levels in the experiment.

The following approximations are made. The spontaneous decay rate back to the metastable levels will be taken to be much smaller than the decay out of the system and can be neglected. (The worst case in yttrium is the ratio of the $^1F_3^\circ\rightarrow{}^1G_4$ transition strength to the $^1F_3^\circ$ total decay strength of $\frac{1}{8}$.[19]) The metastable levels are assumed to be much longer lived than the transit time through the apparatus. All Rabi frequencies and detunings will also be assumed to be much smaller than the upper state decay rate. The result of these approximations is that the population of the excited state is essentially zero ($<1\%$) and constant throughout the process and the total fluorescence can be calculated as the difference between the initial and final populations of the two lower states. With a_2 constant, Eq. (A4) can be used to eliminate a_2 from Eqs. (A3) and (A5). The time evolution of the lower states can be written

$$\dot{a}_1=-\tfrac{1}{2}[\gamma_1 a_1+\Omega_r^*\exp(-i\Delta t)a_3] \ , \tag{A6}$$

$$\dot{a}_3=-\tfrac{1}{2}[\gamma_3 a_3+\Omega_r\exp(i\Delta t)a_1] \ , \tag{A7}$$

with $\gamma_{1,3}=|\Omega_{1,2}|^2/\gamma_2$ and $\Omega_r=\Omega_1\Omega_2^*/\gamma_2$

where $\Delta(\delta_2-\delta_1)$ is the detuning of the two lasers from two-photon resonance. γ_1, γ_3, and Ω_r are the reduced Rabi frequencies of Hemmer.

Solving the two coupled equations gives the following result:

$$|a_1(t)|^2+|a_3(t)|^2=\frac{e^{-(\gamma_1+\gamma_3)t/2}}{|\eta|^2}(|\eta\cosh(\eta t/2)|^2+[\Delta^2+(\gamma_1+\gamma_3)^2/4]|\sinh(\eta t/2)|^2 + (f_1-f_3)\mathrm{Re}\{[2i\Delta-(\gamma_1-\gamma_3)]\eta^*\sinh(\eta t/2)\cosh(\eta^* t/2)\}) \tag{A8}$$

with $\eta=[(\gamma_1+\gamma_3)^2/4-\Delta^2+i\Delta(\gamma_1-\gamma_3)]^{1/2}$ and where f_1 and f_3 are the initial fractional populations of the two lower states.

For a comparison with previous calculations we can take this to the infinite time limit to get, for $\Delta=0$,

$$|a_1(\infty)|^2+|a_3(\infty)|^2=\tfrac{1}{2}\left[1-(f_1-f_3)\frac{1-\varepsilon}{1+\varepsilon}\right] \ , \tag{A9}$$

where $\varepsilon=\gamma_3/\gamma_1$.

In all of our experiments there is no state preparation and both lower states are expected to have equal initial populations, thus the terms in Eqs. (A8) and (A9) which depend on the difference in the populations will vanish. In the case of Eq. (9) the trapping is seen to be 50% in this case. If the sample is prepared initially in state 1 then Eq. (A9) gives $\varepsilon/(1+\varepsilon)$, in agreement with results

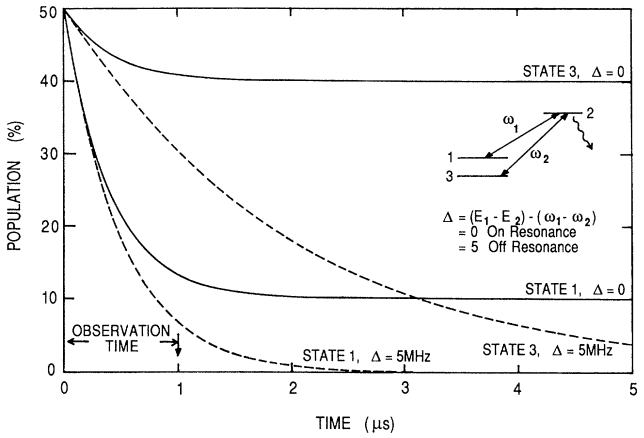

FIG. 6. Time evolution of the two metastable levels both on and off two-photon resonance. The calculations assume a perfect three-level system and are based on typical laser powers and transition strengths. The observation time of 1 μs is the transit time of the ions through the apparatus.

from the dressed state approach for a strongly coupled system[17] in the infinite time limit.

The time evolution, both on and off two-photon resonance, of the individual levels is shown in Fig. 6 for $\varepsilon=0.25$ and a typical low laser power. It can be seen that most of the population is trapped in the more weakly coupled level and that the sum is 0.5 at long times. Making the Rabi frequencies more nearly equal results in a quicker equilibrium being reached and will enhance the signal when interaction times are short.

The FWHM of the dip can be evaluated numerically for Eq. (A8) for a range of laser powers. The result is shown in Fig. 4 of the main text. In this figure the ratio of the two Rabi frequencies is 0.25 but the results are within $\pm 5\%$ for all ratios. In all cases the low-power limit is $0.91/T$ (Hz). This is similar to the two-level Rabi result of $0.8/T$. In the ideal case of a three-level system optimum resolution occurs for low laser power while optimum signal occurs for maximum laser power, however, the linewidth is much less sensitive, allowing reasonable laser power to be used without loss of resolution.

Real systems: more than three levels

The studies made on the Y II $4d^2\ ^1G_4 \rightarrow 4d5p\ ^1F_3^\circ$ transition show qualitatively the expected increase of the linewidth with laser power, however, the increase in depth of the signal was not seen. Earlier studies[6] on the Sc II $3d^2\ ^3P_2 \rightarrow 3d4p\ ^3P_2^\circ$ line did not include studies on the width, due to the short length of the interaction region, but do show the expected increase in the depth with an increase in laser power.

Apart from the interaction regions used for the two atoms, the main difference is the need to include more than three levels in the analysis of yttrium. The upper and lower states of this yttrium transition possess similar hyperfine splittings, 190 and 167 MHz, respectively. Thus a fourth level is only 23 MHz detuned from one of the laser frequencies. This is in contrast to scandium[6] where the nearest upper hyperfine level is 570 MHz detuned. The effect of a near-resonant level is to provide a leak mechanism for the trapped population which effectively shortens the lifetime of the metastable level. Applying the same approximations to the decay rate of this extra excited level the amplitude equations may be written

$$\dot{a}_1 = -\tfrac{1}{2}[\gamma_1 a_1 + \Omega_r^* \exp(-i\Delta t) a_3]\ , \tag{A10}$$

$$\dot{a}_3 = -\tfrac{1}{2}[(\gamma_3+\gamma')a_3 + \Omega_r \exp(i\Delta t) a_1] \tag{A11}$$

with $\gamma' = |\Omega|^2/\gamma_4$. Here, $|\Omega|$ represents the Rabi frequency connecting the extra level as determined by the laser power and detuning, γ_4 is the decay rate of the second upper level, and level 3 is the state that is in near resonance with the extra upper level. When the leak rate is small an approximate solution to this equation may be obtained for the case of exact two-photon resonance which contains an overall factor $\exp(-\gamma' t)$ that eliminates the population trapping as $t \rightarrow \infty$. However, the remainder of the solution is as before and for short times the partial trapping still varies with Δ, but the amplitude of the signal is suppressed. In addition to the loss of signal, light shifts due to the presence of this level will greatly perturb the measurements as the laser power is increased.

[1]J. A. R. Griffith, G. R. Isaak, R. New, M. P. Ralls, and C. P. van Zyl, J. Phys. B **10**, L91 (1977).
[2]J. Mlynek and R. Grimm, Appl. Phys. B **45**, 77 (1988).
[3]M. Kaivola, P. Thorsen, and O. Poulsen, Phys. Rev. A **32**, 207 (1985).
[4]P. R. Hemmer, G. P. Ontai, and S. Ezekiel, J. Opt. Soc. Am. B **3**, 219 (1986).
[5]P. R. Hemmer, M. S. Shahriar, V. D. Natoli, and S. Ezekiel, J. Opt. Soc. Am. B **6**, 1519 (1989).
[6]L. Young, T. Dinneen, and N. B. Mansour, Phys. Rev. A **38**, 3812 (1988).
[7]N. B. Mansour, T. Dinneen, and L. Young, Phys. Rev. A **39**, 5762 (1989).
[8]R. Allison, J. Burns, and A. J. Tuzolino, J. Opt. Soc. Am. **54**, 747 (1964).
[9]R. A. Knapp, Appl. Opt. **2**, 1334 (1963).
[10]W. J. Childs, David R. Cok, L. S. Goodman, and O. Poulsen, Phys. Rev. Lett. **47**, 1389 (1981).
[11]U. Nielsen (private communication).
[12]P. G. H. Sandars and J. Beck, Proc. R. Soc. London, Ser. A **289**, 97 (1965).
[13]Charlotte Froese Fischer, *The Hartree Fock Method for Atoms; A Numerical Approach* (Wiley, New York, 1977).
[14]R. E. Watson and A. J. Freeman, in *Hyperfine Interactions*, edited by A. J. Freeman and R. B. Frankel (Academic, New York, 1967), and references therein.
[15]G. Borghs, P. DeBisschop, J. Odeurs, R. E. Silverans, and M. VanHove, Phys. Rev. A **31**, 1434 (1985).

[16]V. S. Letokov and V. P. Chebotayev, *Nonlinear Laser Spectroscopy* (Springer, New York, 1977).
[17]P. M. Radmore and P. L. Knight, J. Phys. B **15**, 261 (1982).
[18]F. T. Hioe and C. E. Carroll, Phys. Rev. A **37**, 3000 (1988).
[19]*Experimental Transition Probabilities for Spectral Lines of Seventy Elements,* edited by C. H. Corliss and W. R. Bozman, Natl. Bur. Stand. (U.S.) Monograph No. 53 (U.S. GPO, Washington, D.C., 1962).